sustainability

Article

Impact of Shortening Real Driving Emission (RDE) Test Trips on CO, NO_X, and PN_{10} Emissions from Different Vehicles

Haiguang Zhao [1,2], Laihua Shi [3], Xiaoliu Xu [3], Jinshan Qiu [3], Lan Li [3], Junfang Wang [1,2], Wenhan Yu [4,*] and Yunshan Ge [4]

1 State Environmental Protection Key Laboratory of Vehicle Emission Control and Simulation, Chinese Research Academy of Environmental Sciences, Beijing 100012, China; zhaohg@vecc.org.cn (H.Z.); wangjf@vecc.org.cn (J.W.)
2 Vehicle Emission Control Center, Chinese Research Academy of Environmental Sciences, Beijing 100012, China
3 China Merchants Testing Vehicle Technology Research Institute Co., Ltd., Chongqing 401329, China; shilaihua@cmhk.com (L.S.); cjxuxiaoliu@cmhk.com (X.X.); cjqiujinshan@cmhk.com (J.Q.); lilan@cmhk.com (L.L.)
4 National Laboratory of Auto Performance and Emission Test, Beijing Institute of Technology, Beijing 100081, China; geyunshan@bit.edu.cn
* Correspondence: yuwenhan0201@163.com

Abstract: The real driving emission (RDE) test is the test for vehicle type approval in the China VI emission standard and is one of the most important indicators for assessing the environmental performance of vehicles. To investigate the feasibility of shortening the RDE test trip, we measured emissions of CO, NO_X, and PN_{10} (i.e., the number of particles above 10 nm in diameter) from gasoline, diesel, and hybrid electric vehicles based on portable emission measurement systems (PEMSs) and analyzed the influence of shortening test trips on pollutant emissions. The results indicated that the CO and PN_{10} emission factors of the gasoline vehicle increased by about two times during short trips compared with standard trips, while the NO_X emission factor changed insignificantly. The diesel vehicle showed a two-fold increase in NO_X and PN_{10} emission factors during short trips compared with standard trips, with CO emissions remaining largely unchanged. The short trips of the hybrid electric vehicle doubled CO and PN_{10} emission factors and slightly increased NO_X emission factors compared with standard trips. The study can aid in improving RDE test efficiency, reducing RDE test cost, and controlling pollutant emissions from newly produced and in-use vehicles, which is crucial for air pollution management and sustainable development.

Keywords: real driving emission (RDE); short trip; gasoline vehicle; diesel vehicle; hybrid electric vehicle

check for updates

Citation: Zhao, H.; Shi, L.; Xu, X.; Qiu, J.; Li, L.; Wang, J.; Yu, W.; Ge, Y. Impact of Shortening Real Driving Emission (RDE) Test Trips on CO, NO_X, and PN_{10} Emissions from Different Vehicles. *Sustainability* **2024**, *16*, 9453. https://doi.org/10.3390/su16219453

Academic Editor: Ali Bahadori-Jahromi

Received: 30 September 2024
Revised: 24 October 2024
Accepted: 29 October 2024
Published: 30 October 2024

Copyright: © 2024 by the authors. Licensee MDPI, Basel, Switzerland. This article is an open access article distributed under the terms and conditions of the Creative Commons Attribution (CC BY) license (https://creativecommons.org/licenses/by/4.0/).

1. Introduction

In China, the overall number of vehicles has reached 440 million by the end of June 2024 [1] and continues to grow. Previous studies have indicated that the overall number of vehicles will continue to increase to 530–623 million in China in 2050 [2]. This proliferation, while indicative of economic growth and societal advancements, poses a formidable challenge to sustainable development efforts. Based on the data published by the Ministry of Ecology and Environment of the People's Republic of China, the emissions of carbon monoxide (CO), hydrocarbons (HC), nitrogen oxides (NO_X), and particulate matter (PM) from vehicles in China in 2022 were 7430 Gg, 1912 Gg, 5267 Gg, and 53 Gg, respectively [3]. The continuous increase in overall vehicle number has led to vehicle pollution that cannot be ignored [4–8]. Elevated vehicle emissions can cause adverse health effects, including respiratory and cardiovascular diseases and even premature death [9–11]. The emissions not only exacerbate the issue of air pollution but also jeopardize the long-term viability of pursuing a green and sustainable future.

Significant efforts have been made to mitigate the harmful effects of road transportation, and legislation on vehicle emission standards has been enforced globally in the past decades [12,13]. Up to now, the EU emission legislation still dominates the global automotive market, and China's automotive emission regulations are based on the EU legislation [14,15]. After the severe haze event in 2013 [16–18], air pollution control took on an unprecedented importance. This resulted in the accelerated release of the China VI emission standard in 2016 [19], a mere three years after the implementation of the China V emission standard. This rapid progression underscores the nation's resolve to combat air pollution and aligns with its broader environmental sustainability goals. It is crucial to acknowledge that while informative, traditional laboratory-based standard driving cycles are inherently limited in their ability to represent the complexities and nuances of real-world driving conditions. Vehicle emissions are significantly impacted by diverse driving behaviors, road types, traffic congestion, and environmental factors. Some research revealed that standard driving cycles in lab conditions do not accurately represent the driving characteristics of vehicles on real roads, and the emission results obtained differ somewhat from real driving emissions [13,20–22]. For vehicle type approval, the China VI regulation incorporated real driving emission (RDE) tests, marking a significant step towards ensuring more accurate and realistic emissions measurements under real-world driving conditions.

The RDE test involves the utilization of portable emission measurement systems (PEMSs) to measure and evaluate the on-road emission levels of vehicles under real-world conditions of usage [23–25]. This approach offers a more accurate portrayal of emissions behavior than laboratory-based evaluations, as it takes into account the intricate interplay between vehicle performance, usage patterns, and the diverse ambient and driving conditions that inevitably arise in practical applications. While road tests are more reflective of real-world conditions than laboratory tests, even when all possible impact parameters (e.g., fuel, pre-conditioning, weight, etc.) are held constant, the results may show a higher degree of dispersion due to variations in vehicle response and utilization, as well as a wider range of possible environmental and driving conditions [26–29].

Research has demonstrated that experimental conditions (e.g., driving behavior [30,31], vehicle speed [32,33], road grade [34–36], fuel type [37], and ambient conditions [22,25]) have varying degrees of influence on the emission results of real-world on-road experiments. Moreover, it has been demonstrated that pollutant contributions in RDE tests are more dependent on non-temperature conditions, including trip dynamics and route topography [22]. In addition, road grade and altitude are additional realistic driving factors that have a significant influence on vehicle emissions [38,39]. Positive road grades (uphill) resulted in additional loads, and negative road grades (downhill) resulted in reduced loads during vehicle driving [34,40]. At intersections in urban areas, significant emissions are generated due to frequent vehicle stops and delays [31], and frequent stops have a negative impact on the average fuel consumption gap [30]. The RDE test procedure limits the test conditions to prevent large variations in RDE results and the invalidation of the RDE test due to abnormal emissions under extreme conditions [14,27]. These include, but are not limited to, the adoption of a rigorously defined experimental protocol, the specification of approved lubricants and fuels, comprehensive emission assessments, the designation of representative driving routes spanning urban, rural, and motorway domains, and the establishment of precise boundary conditions for test execution.

In the context of sustainable development, the RDE test has emerged as a pivotal metric for assessing the environmental friendliness of vehicles [19]. It represents a cornerstone in the quest for cleaner transportation solutions, underscoring the industry's commitment to reducing vehicle emissions and the adverse effects of vehicular pollution on the environment and public health. As such, RDE has become a focal point for major automobile manufacturers, necessitating significant investments in research and development, personnel resources, and testing capabilities. The pursuit of efficiency and cost-effectiveness in the RDE test is not merely an economic imperative but also a strategic imperative aligned with sustainable development goals. Shortening the test trip represents a targeted approach to enhancing testing efficiency. By optimizing test trips, minimizing unnecessary travel, and leveraging advanced data acquisition and analysis techniques, manufacturers can expedite the testing process while maintaining the rigor and accuracy required to produce meaningful results. However, investigating the effect of shortening the RDE test trip on emission results is critical to determining the feasibility of shortening the RDE test trip. Based on PEMSs, this study tested the CO, NO_X, and PN_{10} (i.e., the number of particles above 10 nm in diameter) emissions from three vehicles (i.e., one gasoline vehicle, one diesel vehicle, and one hybrid electric vehicle) during standard and short trips to investigate the effect of shortening the trip on the RDE emission results, analyzing the changes in CO, NO_X, and PN_{10} emissions of the different vehicles after shortening the RDE trip, and investigating the reasons for the changes in emissions by using time-solved emission data. The results can provide references for the formulation of future emission regulations, help further control vehicle pollution, and promote sustainable development.

2. Materials and Methods

2.1. Vehicle Information

A gasoline vehicle, a diesel vehicle, and a hybrid electric vehicle with the China VIb emission standard were chosen to evaluate the influence of shortening the test trip on CO, NO_X, and PN_{10} emissions from the different vehicles. The tests were conducted in Chongqing, China, based on PEMSs. The main vehicle information is provided in Table 1. All vehicles are well maintained.

Table 1. Main vehicle information.

	Gasoline Vehicle	Diesel Vehicle	Hybrid Electric Vehicle
Vehicle type	N_1 [1]	N_1	M_1 [2]
Curb weight (kg)	1370	2010	2058
Engine type	PFI [3]	GDI [4]	PFI; GDI
Fuel	Gasoline 92#	Diesel 0#	Gasoline 92#
Engine displacement	1.5 L	2.3 T	2.0 T
Odometer (km)	400	4880	3584
Exhaust after-treatment	TWC [5] + GPF [6]	DOC [7] + SDPF [8] + SCR [9] + ASC [10]	TWC + GPF
Emission category	China VIb	China VIb	China VIb

[1] N_1 vehicles are trucks with a maximum gross design mass of not more than 3500 kg [19]. [2] M_1 vehicles are passenger vehicles with a seating capacity of not more than nine seats, including the driver's seat [19]. [3] PFI is port fuel injection. [4] GDI is gasoline direct injection. [5] TWC is three-way catalyst. [6] GPF is gasoline particulate filter. [7] DOC is diesel oxidation catalyst. [8] SDPF is selective catalyst reduction catalyst. [9] SCR is selective catalytic reduction. [10] ASC is ammonia slip catalyst.

2.2. Experimental Section

In this study, two types of mainstream PEMSs (HORIBA OBS-ONE and SENSORS LDV) were employed. Before the tests began, a validation procedure was performed with a chassis dynamometer to ensure that the differences between the PEMSs and the lab analyzers were within the regulations. The PEMS installation is depicted in Figure 1. PEMSs mainly include three parts: a gas analysis module, a particle number (PN) analysis module, and an exhaust flow meter. The condensation particle counter within the PN module, with a PN cut-off size set at 23 nm, was utilized to quantify the PN concentration. The flow meter was used to measure the volume flow rate of exhaust. The weather station documented the ambient conditions. The real-time vehicle parameters (e.g., coolant temperature and engine speed) were captured through the standardized onboard diagnostics protocol. The GPS module tracked the position of the vehicle, and the instantaneous speed was calculated from the GPS data. The PEMS was powered by an additional battery independent of the vehicle's electrical system to minimize any potential impact on vehicle fuel consumption. The comprehensive details regarding the PEMSs can be found in our previous studies [29,41].

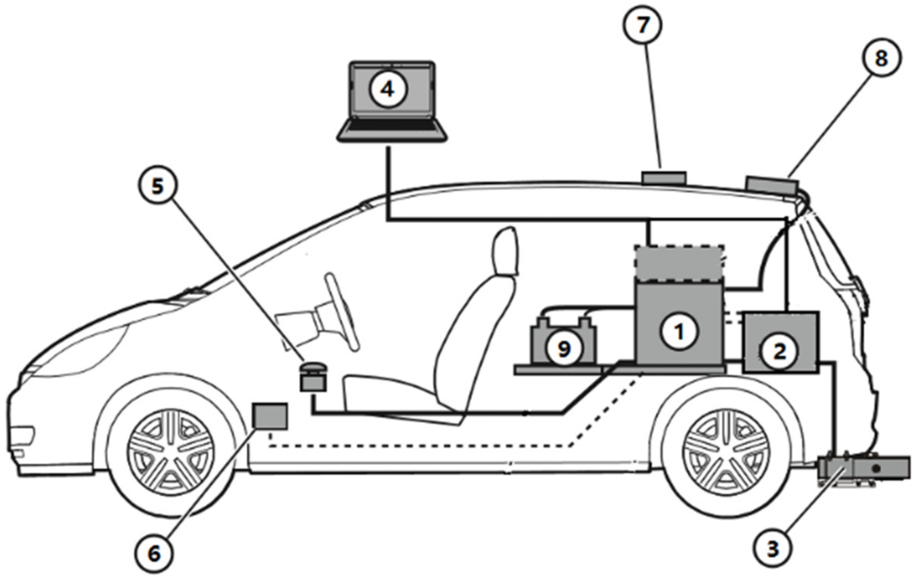

① GAS Analyzer ② PN Module ③ Flow meter ④ Laptop ⑤ Emergency switch
⑥ OBD connector ⑦ GPS ⑧ Weather station ⑨ Battery

Figure 1. Schematic diagram of PEMS installation.

Each vehicle was driven outside of peak hours by a professional driver, with another person on board to oversee the vehicle and the PEMS. Each vehicle was tested twice, one standard trip and one short trip, for a total of six tests. To ensure the cold start phase, the vehicles underwent an overnight soak. Throughout the testing process, the hybrid electric vehicle was used in normal driving mode and operated in a charge-sustaining capacity. The RDE test was conducted in strict accordance with the requirements of the China VI emission standard. In order to minimize systematic errors, the gas analyzer was calibrated before and after the test using standard gases that matched the concentration range of the pollutants in the test vehicle for the zero and range points. In addition, the zero point of the particle analyzer was determined by collecting HEPA-filtered ambient air mounted on the probe before and after the test. The differences in the analyzer check results before and after the test were in compliance with the China VI emission standard. All the data recorded were synchronized in a timely manner.

2.3. Test Routes

Two types of trips (standard and short) were conducted for testing vehicles in Chongqing, China. The standard trip ranged in length from 78.1 km to 80.7 km, while the short trip ranged from 34.2 km to 42.8 km. All the routes tested were compliant with the China VI RDE boundary requirements [19]. Three different types of vehicles were tested on the same route, but it's mentioned that the information displayed in different tests may vary slightly because of GPS drift. Detailed route information and regulation boundaries are listed in Tables 2 and S1. Additionally, the route recorded by GPS on the map for each test is shown in Figures S1 and S2, and the definitions of standard trips, short trips, full trips, and urban trips can be found in Supplementary Materials. Urban trips are part of the test trips, mainly including arterial and secondary trunk roads, with a maximum speed of <60 km/h. The test time avoided the local morning and evening rush hours, and the road conditions were good.

Table 2. The parameter of test routes and regulation boundaries.

Vehicle Type		Gasoline Vehicle		Diesel Vehicle		Hybrid Electric Vehicle		Boundary Requirements [19]
Trip Type		Standard	Short	Standard	Short	Standard	Short	
Total distance (km)		78.1	34.2	80.7	42.8	79.3	37.2	-
Urban portion (%)		33%	31%	33%	26%	33%	33%	29–44
Rural portion (%)		35%	34%	33%	38%	33%	33%	23–43
Motorway portion (%)		32%	35%	34%	36%	34%	34%	23–43
Vehicle speed (km/h)	Urban trip	27.2	26.1	28.1	23.2	27.1	28.2	<60
	Rural trip	74.6	69.9	74.0	73.0	75.6	74.9	60–90
	Motorway trip	98.6	96.1	103.1	101.6	103.4	104.9	>90
Average Altitude (masl)		300.6	321.8	289.1	320.7	294.2	320.7	-
Delta Start/End Altitude (m)		3.3	45.1	35.1	45.2	−17.6	45	<100
Cumulative Positive Elevation (m/100 km)		528.2	714.8	518.0	651.4	501.9	626.0	<1200

2.4. Data Analysis

The instantaneous CO and NO_X emission rate can be calculated by Equation (1):

$$m_{\mathrm{i}} = \rho_{\mathrm{i}} \times c_{\mathrm{i}} \times q \times 10^{-3} \tag{1}$$

where, m_i represents the instantaneous pollutant i (e.g., CO and NO_X) emission rate, g/s; ρ_{i} represents the density of pollutant i, kg/m^3; c_{i} represents the concentration of pollutant i, ppm; and q represents the exhaust flow rate, m^3/s.

The instantaneous PN_{10} emission rate can be calculated using Equation (2):

$$m_{PN_{10}} = c_{PN_{10}} \times q \tag{2}$$

where, $m_{PN_{10}}$ denotes the instantaneous PN_{10} flow rate, #/s; $c_{PN_{10}}$ denotes the concentration of PN_{10}, #/m^3; and q represents the exhaust flow rate, m^3/s.

Based on the distance-specific method, the CO, NO_X, and PN_{10} emission factors were obtained using Equations (3) and (4):

$$EF_i = \frac{\sum m_i}{d} \times 10^3 \tag{3}$$

$$EF_{PN_{10}} = \frac{\sum m_{PN_{10}}}{d} \tag{4}$$

where, EF_i denotes the emission factors of pollutant i, mg/km; m_{i} represents the instantaneous pollutant i (e.g., CO and NO_X) emission rate, g/s; d denotes the distance of test trips, km; $EF_{PN_{10}}$ denotes the emission factors of PN_{10}, #/km; and $m_{PN_{10}}$ denotes the instantaneous PN_{10} flow rate, #/s.

3. Results and Discussions

3.1. Gasoline Vehicle

3.1.1. Standard Trips

Table 3 illustrates CO, NO_X, and PN_{10} emission factors for gasoline, diesel, and hybrid electric vehicles during standard trips. The CO, NO_X, and PN_{10} emission factors for the full trip were 63.47 mg/km, 96.26 mg/km, and 4.81 × 10^{10} #/km, respectively, which complied with the limit values of the China VIb emission standard. Compared with previous studies, the CO emission factor in this study was lower than that of Hu et al. [42] (198.09 mg/km) and the NO_X emission factor was higher than that of Hu et al. [42] (7.2 mg/km). Whereas the PN_{10} emission factor was lower than the studies of Lv et al. [43] (6.0–9.7 × 10^{10} #/km) and He et al. [44] (2.44 × 10^{13} #/km) and between the results of Zhang et al. [45] (1.85–5.25 × 10^{10} #/km). Test method, engine type, and test location contributed to these differences.

Table 3. CO, NO_X, and PN_{10} emission factors for gasoline, diesel, and hybrid electric vehicles during standard trips.

Trip	Pollutant	Emission Factors		
		Gasoline Vehicle	**Diesel Vehicle**	**Hybrid Electric Vehicle**
Full trip	CO (mg/km)	63.47	6.10	224.16
	NO_X (mg/km)	96.26	9.88	8.92
	PN_{10} (×10^9 #/km)	48.07	3.06	3.86
Urban trip	CO (mg/km)	76.67	11.95	82.67
	NO_X (mg/km)	151.10	25.01	11.84
	PN_{10} (×10^9 #/km)	78.96	2.88	5.93

Moreover, the CO, NO_X, and PN_{10} emission factors were higher for urban trips than for full trips, by 20.8%, 57.0%, and 64.3%, respectively. This phenomenon is related to the fact that urban trips include a cold start phase. The reason behind this high percentage is that, during the cold start phase, the engine has not been fully warmed up, resulting in incomplete fuel combustion. This incomplete combustion led to the formation of higher levels of pollutant emissions, including CO, HC, NO_X, etc. Moreover, the low temperature of the engine's oil and other lubricants resulted in increased friction and wear, which could further exacerbate pollutant emissions. In addition, the mainstream exhaust emissions after-treatment technologies, such as three-way catalyst (TWC), selective catalytic reduction (SCR), diesel oxidation catalyst (DOC), and diesel particulate filter (DPF), typically require sufficient temperature to achieve good purification or maintain normal operating conditions [46]. These after-treatment devices may not operate at optimal temperatures during the cold start phase, limiting their effectiveness in converting pollutants. Researchers have revealed that the cold start CO emissions may account for more than 50% of total CO emissions [47–49]. The increase in NO_X and PN_{10} emission factors was greater than that of CO emission factors, suggesting that NO_X and PN_{10} emissions from the gasoline vehicle were more impacted by the cold start phase and road conditions. In addition, in terms of emission values, the emissions of CO, NO_X, and PN_{10} during urban trips accounted for 39.5%, 51.3%, and 53.7% of the total emissions, respectively. The CO, NO_X, and PN_{10} emissions during rural and motorway trips accounted for 60.5%, 48.7%, and 46.3% of the total emissions, respectively. It indicated that gasoline vehicles emit more NO_X and PN_{10} in urban conditions and more CO in rural and motorway conditions.

3.1.2. Short Trips

The emission factors of CO, NO_X, and PN_{10} for the full trips during short trips were also lower than the limit values of the China VIb emission standard by 111.88 mg/km, 92.57 mg/km, and 4.18 × 10^{11} #/km, respectively. The values of CO, NO_X, and PN_{10} emissions during urban trips accounted for 46.8%, 50.7%, and 32.8% of the total emissions for short trips, respectively. The differences in CO, NO_X, and PN_{10} emission factors between standard and short trips for the gasoline vehicle are presented in Figure 2. The CO and PN_{10} emission factors increased approximately two-fold after the shortened test trips compared with the standard trips, while NO_X emission factors showed no significant change. The percentage of NO_X emission values for urban trips in short trips was close to that for standard trips. To explore the reasons for the large changes in CO and PN_{10} emission factors between standard and short trips, we presented time-solved emission data for CO and PN_{10} from the gasoline vehicle in Figures 3 and 4.

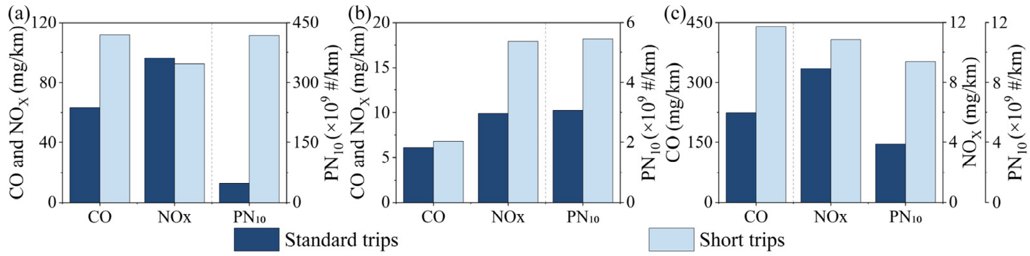

Figure 2. CO, NO_X, and PN_{10} emission factors for (**a**) gasoline, (**b**) diesel, and (**c**) hybrid electric vehicles during standard and short trips.

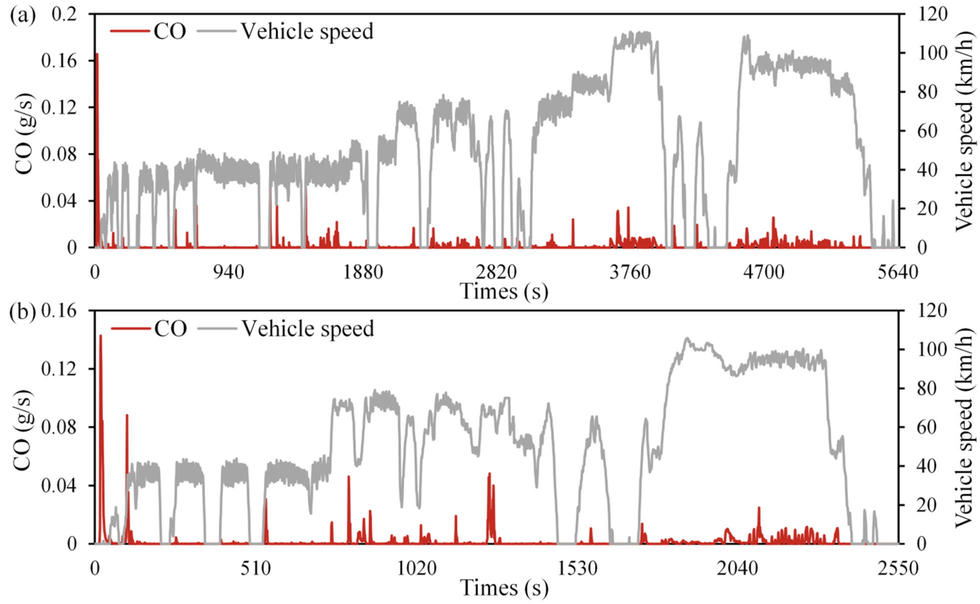

Figure 3. Time-solved CO emissions for the gasoline vehicle on (**a**) standard and (**b**) short trips.

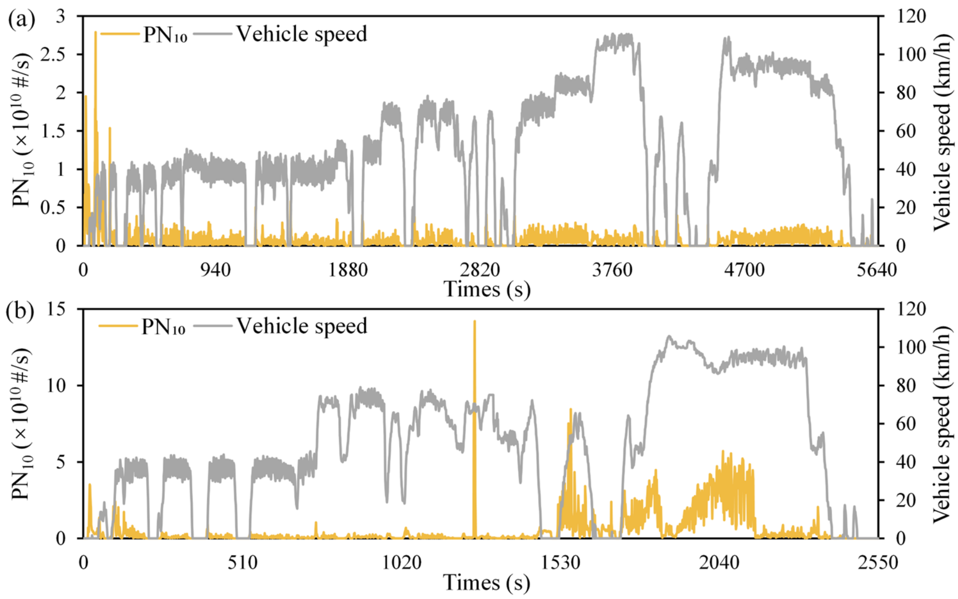

Figure 4. Time-solved PN_{10} emissions for the gasoline vehicle on (**a**) standard and (**b**) short trips.

The high levels of CO emissions observed in both standard and short trips can be predominantly caused by the cold start phase, as well as during certain periods of vehicle acceleration. Moreover, the percentage of CO emission values for urban trips in short trips

(46.8%) was higher than that for standard trips (39.5%). This phenomenon underscores the significance of engine warm-up and efficient acceleration strategies in mitigating emissions. During the cold start phase, when the engine is not fully warmed up, incomplete fuel combustion leads to a disproportionate increase in CO emissions. Specifically, the emission data reveal that the CO emissions generated solely during the cold start phase constitute approximately 25% of the total CO emissions recorded during standard trips and an even more pronounced 28% for short trips. The increase in the CO emission factors for short trips can be attributed to two main factors. First, the total CO emissions during standard and short trips are relatively similar. Second, more critically, the mileage of short trips has been reduced by roughly half, leading to a corresponding reduction in the denominator (i.e., total distance traveled) for calculating the emission factor.

The PN_{10} emission factors for the two trips differed considerably. The increase in the PN_{10} emission factors may be due to the sudden hard braking during the rural trip, which produced very high PN_{10} emissions for a few seconds. Such braking events generate intense friction and heat, leading to the rapid formation and release of fine particles into the atmosphere. In addition, PN_{10} emissions during motorway trips were higher for short trips than during standard trips. On motorway trips, even during short trips, vehicles usually tend to travel at higher speeds and may experience more frequent acceleration and deceleration, which can exacerbate more particle emissions. In addition, most of the vehicles that meet the China VI emission standard currently adopt the automatic start-stop system to enhance the fuel economy of the engine. An automatic start-stop system means that the engine is turned off when the vehicle stops temporarily (e.g., waiting for a green light), and the system automatically restarts the engine when the vehicle must continue. Although the system can decrease the fuel consumption of vehicles, it is possible that the system could lead to higher PN emissions when the vehicle is in real-world operation [50].

3.2. Diesel Vehicle

3.2.1. Standard Trips

The emission factors of CO, NO_X, and PN_{10} from the diesel vehicle during standard trips are shown in Table 3. The emission factors of CO, NO_X, and PN_{10} for the full trip were 6.10 mg/km, 9.88 mg/km, and 3.06×10^9 #/km, respectively, all of which meet the limit values of the China VIb emission standard. The NO_X emission factor in this study was lower than that of Euro 6b light-duty diesel trucks in Korea studied by Ro et al. [51] (550–1830 mg/km). Moreover, the emission factors of CO and NO_X were higher for the urban trip than for the full trip. On the contrary, the emission factors of PN_{10} for the urban trip were lower than those for the full trip. This observation suggests that PN_{10} emissions from the diesel vehicle may be less affected by the cold start phase. In particular, the emission factors of NO_X for the diesel vehicle increased more than the emission factors of CO, indicating that NO_X emissions were more influenced by the cold start phase and road conditions compared with CO emissions. In addition, in terms of emission values, the urban trip accounted for 64.3%, 83.1%, and 30.9% of the total CO, NO_X, and PN_{10} emissions, respectively. Rural trips and motorway trips accounted for 35.7%, 16.9%, and 69.1% of the total CO, $NO_{X,}$ and PN_{10} emissions, respectively. This indicated that diesel vehicles emit more CO and NO_X in urban areas and more PN_{10} in rural areas and motorways. These findings highlight the need for targeted emission reduction policies for different driving environments.

3.2.2. Short Trips

The emission factors of CO, NO_X, and PN_{10} for the full trips during short trips were 6.77 mg/km, 17.87 mg/km, and 5.44×10^9 #/km, respectively, all of which meet the limit of the China VIb emission standard. The values of CO, NO_X, and PN_{10} emissions during urban trips accounted for 81.4%, 83.0%, and 14.8% of the total emissions for short trips, respectively. The differences in CO, NO_X, and PN_{10} emission factors between standard and short trips for the diesel vehicle are indicated in Figure 2. Notably, after reducing the length of the test trips, the emission factors of NO_X and PN_{10} exhibited an approximately two-fold increase compared with the standard trips. In contrast, the CO emission factors remained relatively unchanged, indicating that the duration of the trip may have a lesser impact on CO emissions from the diesel vehicle.

Figures 5 and 6 present the time-solved emission data for NO_X and PN_{10} from the diesel vehicle. Figure 5 reveals that the increase in NO_X emissions for both standard and short trips occurred primarily in the cold start phase and the urban trip. Similar to the CO emission factor for the gasoline vehicle during short trips, the increase in the NO_X emission factor from the diesel vehicle during short trips was caused by the closeness of the total NO_X emissions for the standard and short trips, as well as the halving of the mileage traveled.

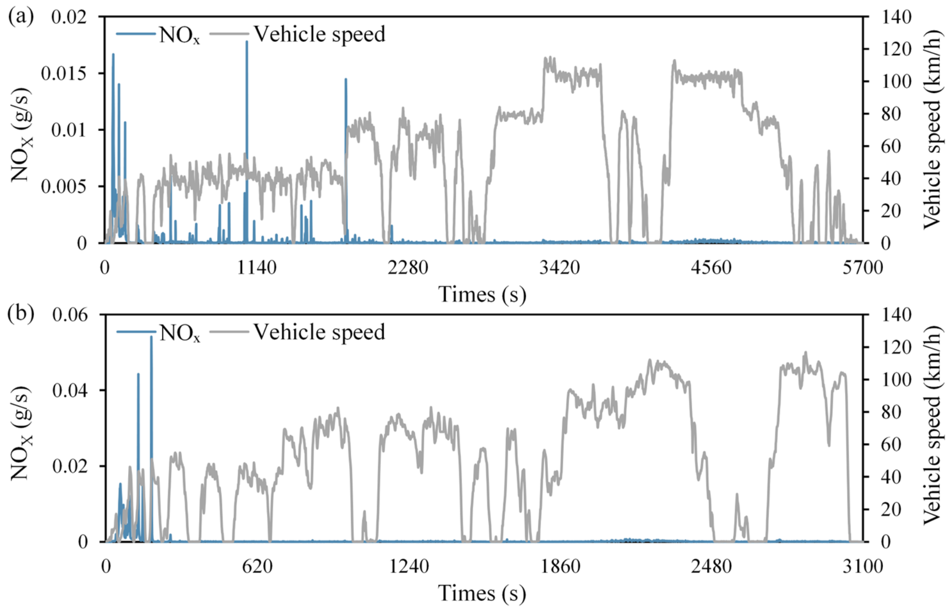

Figure 5. Time-solved NO_X emissions for the diesel vehicle on (**a**) standard and (**b**) short trips.

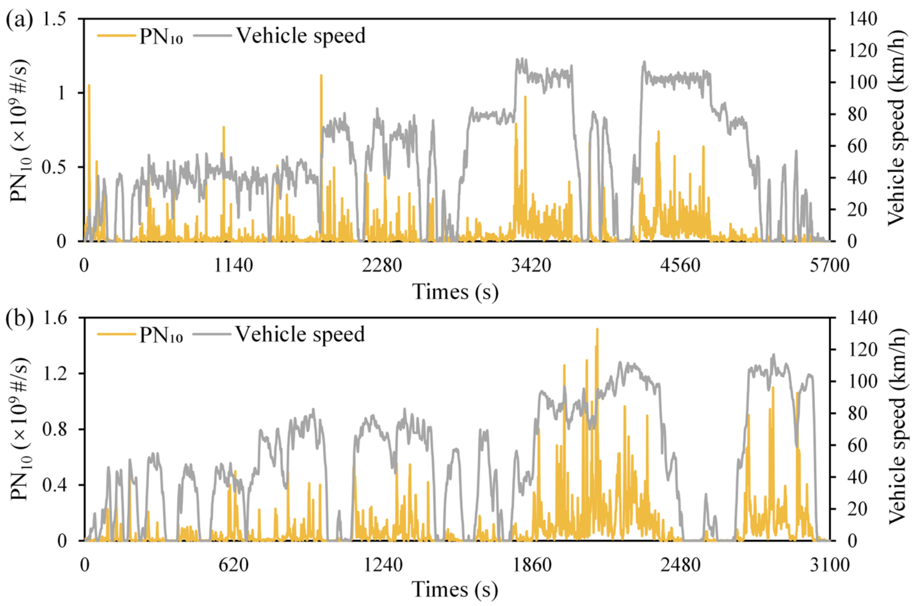

Figure 6. Time-solved PN_{10} emissions for the diesel vehicle on (**a**) standard and (**b**) short trips.

In addition, as illustrated in Figure 6, the PN_{10} emission factors were notably elevated during the motorway trip of the short trips. However, the percentage of PN_{10} emission values for urban trips in short trips (14.8%) was significantly lower than that for standard trips (30.9%). This observation indicated that short trips have more PN_{10} emissions during rural and motorway trips. Under specific driving conditions, such as those encountered on motorways, there is a tendency for higher PN_{10} emissions from diesel vehicles. These conditions include factors like increased vehicle speeds, acceleration, and deceleration, which can affect the combustion process and the particle emissions subsequently.

3.3. Hybrid Electric Vehicle

3.3.1. Standard Trips

The emission factors of CO, NO_X, and PN_{10} for the hybrid electric vehicle during standard trips are shown in Table 3. The emission factors of CO, NO_X, and PN_{10} for the full trip were 224.16 mg/km, 8.92 mg/km, and 3.86×10^9 #/km, respectively, all of which comply with the limits of the China VIb emission standard. The CO and NO_X emission factors in this study were slightly higher than those in studies by Jaworski et al. [52] (195.5 mg/km and 3 mg/km), Skobiej and Pielecha [53] (92.4 mg/km and 5.03 mg/km), and Zheng et al. [54] (154.8 mg/km and 2.7 mg/km), and the PN_{10} emission factor was lower than those by Skobiej and Pielecha [53] (5.43×10^{11} #/km) and Zheng et al. [54] (2.45×10^{11} #/km).

Additionally, the CO emission factor for the urban trip (82.67 mg/km) was lower than that for the full trip. In contrast, the NO_X and PN_{10} emission factors for the urban trip were higher than those for the full trip due to the fact that the hybrid electric vehicle was powered more by electric energy during the urban trip. The researchers found that hybrid electric vehicles had significantly higher PN emissions during cold starts compared with hot starts [45]. Furthermore, in terms of emission values, the urban trip accounted for 12.0%, 43.2%, and 50.0% of total CO, NO_X, and PN_{10} emissions, respectively. Rural trips and motorway trips accounted for 88.0%, 56.8%, and 50.0% of total CO, NO_X, and PN_{10} emissions, respectively. Specifically, the hybrid electric vehicle produced relatively low CO emissions in urban areas, suggesting a potential advantage of hybrid electric vehicles in mitigating urban air pollution. Emissions of NO_X and PN_{10} were comparable in urban, as well as rural, and motorway areas.

3.3.2. Short Trips

The emission factors of CO, NO_X, and PN_{10} for the full trips during short trips were 440.42 mg/km, 10.83 mg/km, and 9.37×10^9 #/km, respectively, all of which meet the limit values of the China VIb emission standard. The values of CO, NO_X, and PN_{10} emissions during urban trips accounted for 17.2%, 48.6%, and 56.5% of the total emissions for short trips, respectively. The differences in CO, NO_X, and PN_{10} emission factors between standard and short trips for the hybrid electric vehicle are presented in Figure 2. Compared with the standard trip, the shortened test trip resulted in approximately a two-fold increase in the CO and PN_{10} emission factors and a slight increase in the NO_X emission factor. Moreover, the short and standard trips have similar emission percentages of CO, NO_X, and PN_{10} for urban trips.

The time-solved emission data for CO, NO_X, and PN_{10} from the hybrid electric vehicle are demonstrated in Figures 7–9. The increase in CO emissions for both standard and short trips occurred mainly at the cold start phase and the urban trip, as shown in Figure 7. The hybrid electric vehicle increased the CO emission factor during short trips for the same reasons as the gasoline vehicle, i.e., close total CO emissions and reduced mileage. In addition, the increase in the PN_{10} emission factor was attributed to the very high PN_{10} emissions for a few seconds during the cold start phase and the motorway trips during short trips, and the total PN_{10} emissions were close to those of the standard and short trips. The increase in NO_X emission factors for short trips was relatively low compared with CO and PN_{10} emission factors, with NO_X emissions of 0.71 g and 0.40 g for standard and short trips, respectively. Furthermore, the NO_X emissions all occurred mainly during the cold start phase, vehicle acceleration, and motorway trips. It showed that the shortened trip had a lower impact on the NO_X emission factor of the hybrid electric vehicle compared with CO and PN_{10} emission factors.

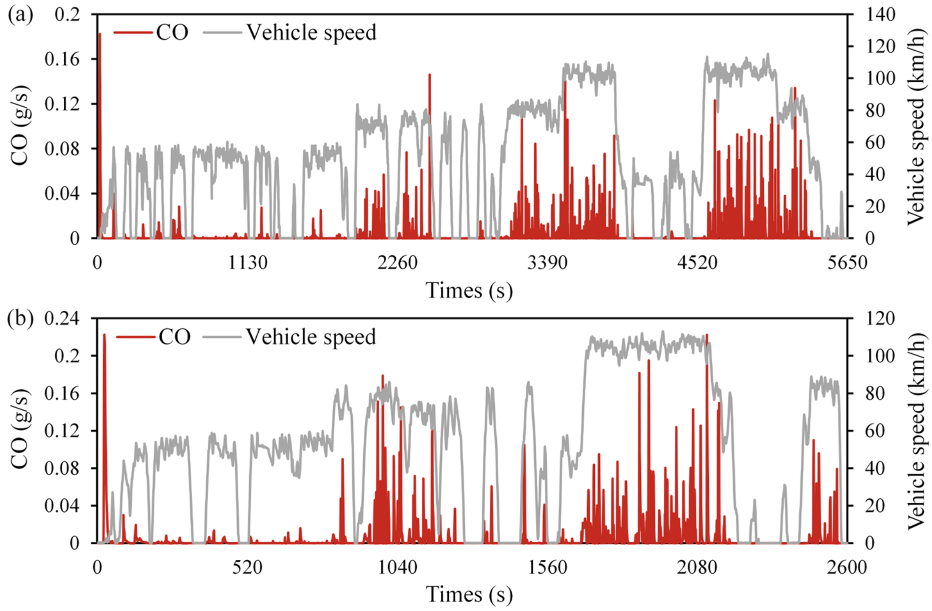

Figure 7. Time-solved CO emissions for the hybrid electric vehicle on (**a**) standard and (**b**) short trips.

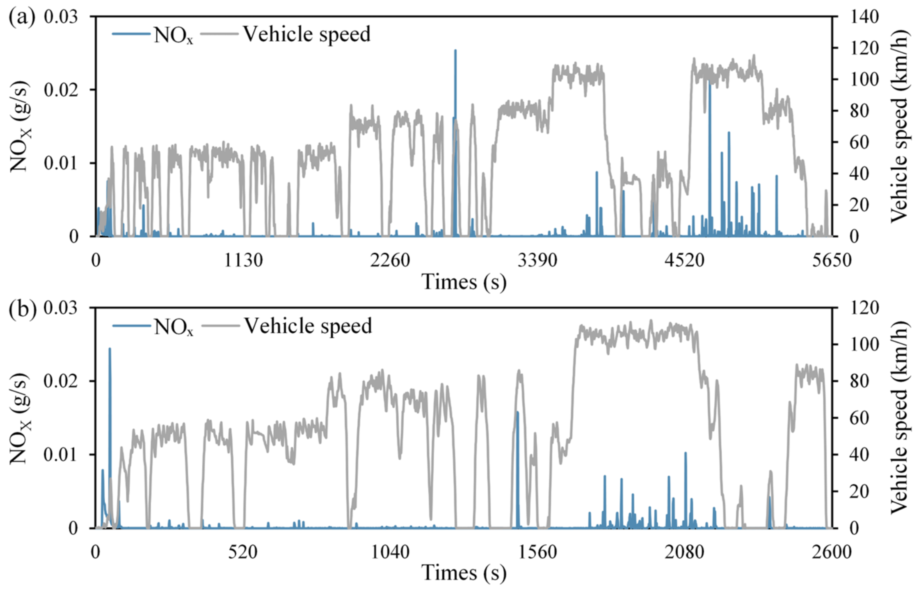

Figure 8. Time-solved NO_X emissions for the hybrid electric vehicle on (**a**) standard and (**b**) short trips.

In addition, it is noteworthy that the transient emissions of CO, NO_X, and PN_{10} during acceleration periods were more prominent in hybrid electric vehicles than in gasoline and diesel vehicles. This phenomenon may be due to the powertrain of the hybrid electric vehicle switches from electric to fuel mode during the acceleration process. At this time the supply of gasoline increases rapidly. However, this sudden increase in the amount of gasoline made it difficult to fully combust in a short period, leading to increased incomplete combustion and higher instantaneous pollutant emissions.

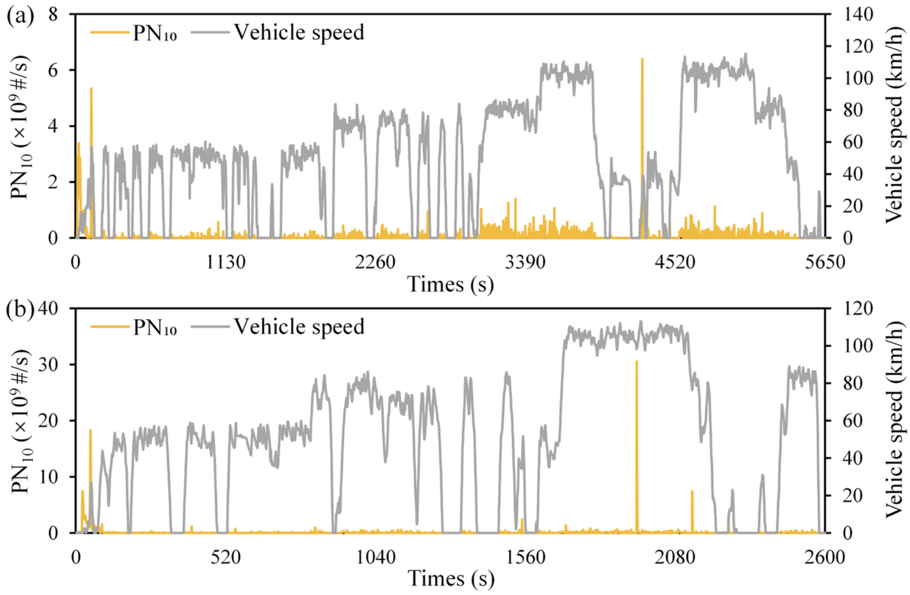

Figure 9. Time-solved PN_{10} emissions for the hybrid electric vehicle on (**a**) standard and (**b**) short trips.

4. Conclusions

Shortening the RDE test trip can enhance the test efficiency, lower test costs, and better reflect the significant impact of cold starts on emissions results. To determine the feasibility of shortening the test trip for the RDE test and to explore the effect of shortened test trips on CO, NO_X, and PN_{10} emissions, we measured the emissions of CO, NO_X, and PN_{10} from gasoline, diesel, and hybrid electric vehicles based on PEMSs for standard and short trips. The main conclusions obtained are as follows:

The emission factors of CO, NO_X, and PN_{10} conformed to the China VIb emission standard for both standard and short trips, indicating that shortening the test trip of RDE may not affect the type approval results of vehicles. However, in terms of the pollutant emission factors, the shortening of trips had an impact on the pollutant emission factors of different vehicles. For the gasoline vehicle, compared with the standard trip, the CO and PN_{10} emission factors for the short trip increased by about two times, while the NO_X emission factor was not significantly changed. For the diesel vehicle, the NO_X and PN_{10} emission factors for short trips increased approximately twice compared with those of the standard trips, while the CO emission factor was not changed significantly. For the hybrid electric vehicle, the shortened test trips led to approximately a two-fold increase in the CO and PN_{10} emission factors and slight increases in NO_X emission factors compared with the standard trip.

The results demonstrate that shortening the test trip of the RDE affected the CO, NO_X, and PN_{10} emissions differently for different vehicles. In future studies, it can be systematically evaluated whether to shorten the test trip of the RDE for the types of pollutants that need to be emphasized in the test. Such a targeted approach has the potential to not only streamline testing procedures and mitigate costs but also to align with the broader goals of promoting sustainable development within the automotive and transportation industries. In addition, the differences in vehicle pollutant emissions in this study also indicate that it is important to explore the causes of pollutant emissions from multiple perspectives, such as engine performance, driving behavior, and road conditions. Moreover, this study has some limitations in terms of sample size. Future studies can increase the sample size, thereby improving the accuracy of the test results. Furthermore, vehicle pollutant emissions can be reduced by promoting smoother driving strategies, optimizing engine calibration during cold start and acceleration phases, and investing in infrastructure improvements (e.g., the use of dust-suppressing materials and improved pavement design). These measures, combined with cleaner vehicle technologies that are being developed, can help reduce the effects of vehicle pollutant emissions on human health and the environment and contribute to sustainable development.

The views expressed in this study may not be regarded as the official position of the authority.

Supplementary Materials: The following supporting information can be downloaded at https://www.mdpi.com/article/10.3390/su16219453/s1.

Author Contributions: Conceptualization, H.Z., W.Y. and Y.G.; Methodology, X.X., J.W., W.Y. and Y.G.; Validation, J.Q. and J.W.; Formal Analysis, H.Z.; Investigation, H.Z.; Resources, X.X.; Data Curation, L.S. and J.Q.; Writing—Original Draft Preparation, H.Z. and W.Y.; Writing—Review and Editing, H.Z., L.S., L.L. and W.Y.; Visualization, H.Z., L.S. and W.Y.; Supervision, W.Y. and Y.G.; Project Administration, H.Z., X.X., L.L. and J.W.; Funding Acquisition, H.Z. All authors have read and agreed to the published version of the manuscript.

Funding: This work was supported by the National Key Research and Development Program of China (No. 2022YFC3703604).

Institutional Review Board Statement: Not applicable.

Informed Consent Statement: Not applicable.

Data Availability Statement: The data presented in this study are available on request from the corresponding author.

Conflicts of Interest: Author Laihua Shi, Xiaoliu Xu, Jinshan Qiu, Lan Li were employed by the company China Merchants Testing Vehicle Technology Research Institute Co., Ltd. The remaining authors declare that the research was conducted in the absence of any commercial or financial relationships that could be construed as a potential conflict of interest.

References

1. Ministry of Public Security of the People's Republic of China. National Vehicle Population Reached 440 Million Vehicles. Drivers Amounted to 532 Million. 2024. Available online: https://www.gov.cn/lianbo/bumen/202407/content_6961935.htm (accessed on 25 September 2024).
2. Huo, H.; Wang, M. Modeling Future Vehicle Sales and Stock in China. *Energy Policy* **2012**, *43*, 17–29. [CrossRef]
3. Ministry of Ecology and Environment of the People's Republic of China. China Mobile Source Environmental Management Annual Report. 2023. Available online: https://www.mee.gov.cn/hjzl/sthjzk/ydyhjgl/202312/W020231211531753967096.pdf (accessed on 25 September 2024).
4. Zhang, Y.; Yang, X.; Wang, Y.; Yang, Z.; Zhao, H.; Ding, Y. Light-Duty Vehicle Organic Gas Emissions from Tailpipe and Evaporation: A Review of Influencing Factors. *Sci. Total Environ.* **2024**, *947*, 174523. [CrossRef] [PubMed]
5. Cao, J.; Liu, J.; Cheng, Y.; Ai, S.; Li, F.; Xue, T.; Zhang, Q.; Zhu, T. Impacts of Different Vehicle Emissions on Ozone Levels in Beijing: Insights into Source Contributions and Formation Processes. *Environ. Int.* **2024**, *191*, 109002. [CrossRef] [PubMed]
6. Wang, M.; Tian, P.; Wang, L.; Yu, Z.; Du, T.; Chen, Q.; Guan, X.; Guo, Y.; Zhang, M.; Tang, C.; et al. High Contribution of Vehicle Emissions to Fine Particulate Pollutions in Lanzhou, Northwest China Based on High-Resolution Online Data Source Appointment. *Sci. Total Environ.* **2021**, *798*, 149310. [CrossRef]
7. Liu, S.; Li, H.; Kun, W.; Zhang, Z.; Wu, H. How Do Transportation Influencing Factors Affect Air Pollutants from Vehicles in China? Evidence from Threshold Effect. *Sustainability* **2022**, *14*, 9402. [CrossRef]
8. Wang, J.; Xu, Z.; Lu, W.; Ding, Y.; Wang, Y.; Hao, L.; Ge, Y. Emission Durability of a China-6 Light-Duty Gasoline Vehicle. *Sustainability* **2024**, *16*, 7526. [CrossRef]
9. McCaffery, C.; Zhu, H.; Li, C.; Durbin, T.D.; Johnson, K.C.; Jung, H.; Brezny, R.; Geller, M.; Karavalakis, G. On-Road Gaseous and Particulate Emissions from GDI Vehicles with and without Gasoline Particulate Filters (GPFs) Using Portable Emissions Measurement Systems (PEMS). *Sci. Total Environ.* **2020**, *710*, 136366. [CrossRef]
10. Bates, J.T.; Weber, R.J.; Abrams, J.; Verma, V.; Fang, T.; Klein, M.; Strickland, M.J.; Sarnat, S.E.; Chang, H.H.; Mulholland, J.A.; et al. Reactive Oxygen Species Generation Linked to Sources of Atmospheric Particulate Matter and Cardiorespiratory Effects. *Environ. Sci. Technol.* **2015**, *49*, 13605–13612. [CrossRef]
11. Kampa, M.; Castanas, E. Human Health Effects of Air Pollution. *Environ. Pollut.* **2008**, *151*, 362–367. [CrossRef]
12. Li, W.; Dong, Z.; Miao, L.; Wu, G.; Deng, Z.; Zhao, J.; Huang, W. On-Road Evaluation and Regulatory Recommendations for NOx and Particle Number Emissions of China VI Heavy-Duty Diesel Trucks: A Case Study in Shenzhen. *Sci. Total Environ.* **2024**, *928*, 172427. [CrossRef]

13. Rexeis, M.; Hausberger, S. Trend of Vehicle Emission Levels until 2020—Prognosis Based on Current Vehicle Measurements and Future Emission Legislation. *Atmos. Environ.* **2009**, *43*, 4689–4698. [CrossRef]
14. Hooftman, N.; Messagie, M.; Van Mierlo, J.; Coosemans, T. A Review of the European Passenger Car Regulations—Real Driving Emissions vs Local Air Quality. *Renew. Sustain. Energy Rev.* **2018**, *86*, 1–21. [CrossRef]
15. Ministry of Ecology and Environment of the People's Republic of China. Limits and Measurement Methods for Emissions from Light-Duty Vehicles (I). 2001. Available online: https://www.mee.gov.cn/image20010518/1920.pdf (accessed on 25 September 2024).
16. Tian, S.; Pan, Y.; Liu, Z.; Wen, T.; Wang, Y. Size-Resolved Aerosol Chemical Analysis of Extreme Haze Pollution Events during Early 2013 in Urban Beijing, China. *J. Hazard. Mater.* **2014**, *279*, 452–460. [CrossRef] [PubMed]
17. Tao, M.; Chen, L.; Xiong, X.; Zhang, M.; Ma, P.; Tao, J.; Wang, Z. Formation Process of the Widespread Extreme Haze Pollution over Northern China in January 2013: Implications for Regional Air Quality and Climate. *Atmos. Environ.* **2014**, *98*, 417–425. [CrossRef]
18. Wang, H.; Tan, S.C.; Wang, Y.; Jiang, C.; Shi, G.Y.; Zhang, M.X.; Che, H.Z. A Multisource Observation Study of the Severe Prolonged Regional Haze Episode over Eastern China in January 2013. *Atmos. Environ.* **2014**, *89*, 807–815. [CrossRef]
19. Ministry of Ecology and Environment of the People's Republic of China. Limits and Measurement Methods for Emissions from Light-Duty Vehicles (CHINA 6). 2016. Available online: https://www.mee.gov.cn/ywgz/fgbz/bz/bzwb/dqhjbh/dqydywrwpfbz/201612/W020171207355626647621.pdf (accessed on 25 September 2024).
20. Huang, R.; Ni, J.; Zheng, T.; Wang, Q.; Shi, X.; Cheng, Z. Characterizing and Assessing the Fuel Economy, Particle Number and Gaseous Emissions Performance of Hybrid Electric and Conventional Vehicles under Different Driving Modes. *Atmos. Pollut. Res.* **2022**, *13*, 101597. [CrossRef]
21. Valverde, V.; Mora, B.A.; Clairotte, M.; Pavlovic, J.; Suarez-Bertoa, R.; Giechaskiel, B.; Astor, C.; Fontaras, G. Emission Factors Derived from 13 Euro 6b Light-Duty Vehicles Based on Laboratory and on-Road Measurements. *Atmosphere* **2019**, *10*, 243. [CrossRef]
22. Wang, R.; Zhang, L.; Peng, J.; Han, J.; Du, B.; Gong, B.; Xue, H.; Tuo, D.; Zhang, Q. Effect of Ambient High-Temperature on Real Driving Emission Tests of a Light-Duty Gasoline Vehicle. *Atmos. Pollut. Res.* **2024**, *15*, 101998. [CrossRef]
23. Huang, C.; Lou, D.; Hu, Z.; Feng, Q.; Chen, Y.; Chen, C.; Tan, P.; Yao, D. A PEMS Study of the Emissions of Gaseous Pollutants and Ultrafine Particles from Gasoline- and Diesel-Fueled Vehicles. *Atmos. Environ.* **2013**, *77*, 703–710. [CrossRef]
24. Kousoulidou, M.; Fontaras, G.; Ntziachristos, L.; Bonnel, P.; Samaras, Z.; Dilara, P. Use of Portable Emissions Measurement System (PEMS) for the Development and Validation of Passenger Car Emission Factors. *Atmos. Environ.* **2013**, *64*, 329–338. [CrossRef]
25. Du, B.; Zhang, L.; Geng, Y.; Zhang, Y.; Xu, H.; Xiang, G. Testing and Evaluation of Cold-Start Emissions in a Real Driving Emissions Test. *Transp. Res. D Transp. Environ.* **2020**, *86*, 102447. [CrossRef]
26. Joumard, R.; Laurikko, J.; Han, T.L.; Geivanidis, S.; Samaras, Z.; Merétei, T.; Devaux, P.; André, J.M.; Cornelis, E.; Lacour, S.; et al. Accuracy of Exhaust Emission Factor Measurements on Chassis Dynamometer. *J. Air Waste Manag. Assoc.* **2009**, *59*, 695–703. [CrossRef]
27. Giechaskiel, B.; Valverde, V.; Melas, A.; Clairotte, M.; Bonnel, P.; Dilara, P. Comparison of the Real-Driving Emissions (RDE) of a Gasoline Direct Injection (GDI) Vehicle at Different Routes in Europe. *Energies* **2024**, *17*, 1308. [CrossRef]
28. Giechaskiel, B.; Clairotte, M.; Valverde-Morales, V.; Bonnel, P.; Kregar, Z.; Franco, V.; Dilara, P. Framework for the Assessment of PEMS (Portable Emissions Measurement Systems) Uncertainty. *Environ. Res.* **2018**, *166*, 251–260. [CrossRef]
29. Wang, Y.; Wang, J.; Hao, C.; Wang, X.; Li, Q.; Zhai, J.; Ge, Y.; Hao, L.; Tan, J. Characteristics of Instantaneous Particle Number (PN) Emissions from Hybrid Electric Vehicles under the Real-World Driving Conditions. *Fuel* **2021**, *286*, 119466. [CrossRef]
30. Pavlovic, J.; Fontaras, G.; Ktistakis, M.; Anagnostopoulos, K.; Komnos, D.; Ciuffo, B.; Clairotte, M.; Valverde, V. Understanding the Origins and Variability of the Fuel Consumption Gap: Lessons Learned from Laboratory Tests and a Real-Driving Campaign. *Environ. Sci. Eur.* **2020**, *32*, 53. [CrossRef]
31. Jang, S.; Song, K.H.; Kim, D.; Ko, J.; Lee, S.M.; Elkosantini, S.; Suh, W. Road-Section-Based Analysis of Vehicle Emissions and Energy Consumption. *Sustainability* **2023**, *15*, 4421. [CrossRef]
32. Bodisco, T.; Zare, A. Practicalities and Driving Dynamics of a Real Driving Emissions (RDE) Euro 6 Regulation Homologation Test. *Energies* **2019**, *12*, 2306. [CrossRef]
33. Vlachos, T.G.; Bonnel, P.; Perujo, A.; Weiss, M.; Villafuerte, P.; Riccobono, F. In-Use Emissions Testing with Portable Emissions Measurement Systems (PEMS) in the Current and Future European Vehicle Emissions Legislation: Overview, Underlying Principles and Expected Benefits. *SAE Int. J. Commer. Veh.* **2014**, *7*, 199–215. [CrossRef]
34. Costagliola, M.A.; Costabile, M.; Prati, M.V. Impact of Road Grade on Real Driving Emissions from Two Euro 5 Diesel Vehicles. *Appl. Energy* **2018**, *231*, 586–593. [CrossRef]
35. Gallus, J.; Kirchner, U.; Vogt, R.; Benter, T. Impact of Driving Style and Road Grade on Gaseous Exhaust Emissions of Passenger Vehicles Measured by a Portable Emission Measurement System (PEMS). *Transp. Res. D Transp. Environ.* **2017**, *52*, 215–226. [CrossRef]
36. Fan, J.; Najafi, A.; Sarang, J.; Li, T. Analyzing and Optimizing the Emission Impact of Intersection Signal Control in Mixed Traffic. *Sustainability* **2023**, *15*, 16118. [CrossRef]

37. Yuan, W.; Frey, H.C.; Wei, T.; Rastogi, N.; VanderGriend, S.; Miller, D.; Mattison, L. Comparison of Real-World Vehicle Fuel Use and Tailpipe Emissions for Gasoline-Ethanol Fuel Blends. *Fuel* **2019**, *249*, 352–364. [CrossRef]
38. Kim, W.G.; Kim, C.K.; Lee, J.T.; Kim, J.S.; Yun, C.W.; Yook, S.J. Fine Particle Emission Characteristics of a Light-Duty Diesel Vehicle According to Vehicle Acceleration and Road Grade. *Transp. Res. D Transp. Environ.* **2017**, *53*, 428–439. [CrossRef]
39. Wang, X.; Yin, H.; Ge, Y.; Yu, L.; Xu, Z.; Yu, C.; Shi, X.; Liu, H. On-Vehicle Emission Measurement of a Light-Duty Diesel van at Various Speeds at High Altitude. *Atmos. Environ.* **2013**, *81*, 263–269. [CrossRef]
40. Della, R.L.; Giovanni, M. The Influence of Road Gradient in an Integrated Approach of Real Driving Cycles and Emissions Factors Model. *Transp. Res. Procedia* **2016**, *14*, 3179–3188.
41. Wang, Y.; Feng, X.; Zhao, H.; Hao, C.; Hao, L.; Tan, J.; Wang, X.; Yin, H.; Wang, J.; Ge, Y.; et al. Experimental Study of CO_2 and Pollutant Emission at Various Altitudes: Inconsistent Results and Reason Analysis. *Fuel* **2022**, *307*, 121801. [CrossRef]
42. Hu, L.; Quan, Y.; Song, B.; Hu, Z. Experimental investigation on emission characteristics from a gasoline direct injection light-duty vehicle certified to meet China VI regulation. *Acta Sci. Circumstantiae* **2018**, *38*, 3496–3502. [CrossRef]
43. Lv, Z.; Peng, J.; Zhang, J.; Yang, L.; Guo, D.; Wei, N.; Wu, Y.; Fang, T.; Song, A.; Fan, C.; et al. Particulate Emissions from Gasoline Vehicles Using Three Different Fuel Injection Technologies. *J. Clean. Prod.* **2023**, *418*, 138123. [CrossRef]
44. He, L.; Hu, J.; Zhang, S.; Wu, Y.; Zhu, R.; Zu, L.; Bao, X.; Lai, Y.; Su, S. The Impact from the Direct Injection and Multi-Port Fuel Injection Technologies for Gasoline Vehicles on Solid Particle Number and Black Carbon Emissions. *Appl. Energy* **2018**, *226*, 819–826. [CrossRef]
45. Zhang, Y.; Yang, X.; Fu, M. Emission Characteristics of Particle Number from Conventional Gasoline and Hybrid Vehicles. *Sustainability* **2024**, *16*, 12. [CrossRef]
46. Li, K.; Xiao, B.; Wang, Y.; Jia, J.; Wu, X. Applications of Electric Heating Technology in Vehicle Exhaust Pollution Control. *Processes* **2024**, *12*, 298. [CrossRef]
47. Reiter, M.S.; Kockelman, K.M. The Problem of Cold Starts: A Closer Look at Mobile Source Emissions Levels. *Transp. Res. D Transp. Environ.* **2016**, *43*, 123–132. [CrossRef]
48. Zhai, Z.; Xu, J.; Zhang, M.; Wang, A.; Hatzopoulou, M. Quantifying Start Emissions and Impact of Reducing Cold and Warm Starts for Gasoline and Hybrid Vehicles. *Atmos. Pollut. Res.* **2023**, *14*, 101646. [CrossRef]
49. Jiang, Y.; Song, G.; Wu, Y.; Lu, H.; Zhai, Z.; Yu, L. Impacts of Cold Starts and Hybrid Electric Vehicles on On-Road Vehicle Emissions. *Transp. Res. D Transp. Environ.* **2024**, *126*, 104011. [CrossRef]
50. Yu, F.; Zhong, Z.; Wang, Q.; Liao, S.; Zhu, M.; Sha, Q.; Liu, J.; Zheng, J. Characterizing the Particle Number Emissions of Light-Duty Gasoline Vehicles under Different Engine Technologies and Driving Conditions. *Environ. Res.* **2022**, *213*, 113648. [CrossRef]
51. Ro, S.; Park, J.; Shin, M.; Lee, J. Developing On-Road NOx Emission Factors for Euro 6b Light-Duty Diesel Trucks in Korean Driving Conditions. *Energies* **2021**, *14*, 1041. [CrossRef]
52. Jaworski, A.; Kuszewski, H.; Lew, K.; Wojewoda, P.; Balawender, K.; Woś, P.; Longwic, R.; Boichenko, S. Assessment of the Effect of Road Load on Energy Consumption and Exhaust Emissions of a Hybrid Vehicle in an Urban Road Driving Cycle—Comparison of Road and Chassis Dynamometer Tests. *Energies* **2023**, *16*, 5723. [CrossRef]
53. Skobiej, K.; Pielecha, J. Analysis of the Exhaust Emissions of Hybrid Vehicles for the Current and Future RDE Driving Cycle. *Energies* **2022**, *15*, 8691. [CrossRef]
54. Zheng, F.; Zhao, H.; Ji, J.; Yin, H.; Ding, Y.; Li, J. Real Driving Emission Characteristics of China VI Hybrid Electric Vehicle Based on Altitude Conditions in Beijing and Kunming. *Res. Environ. Sci.* **2022**, *35*, 1581–1588. [CrossRef]

Disclaimer/Publisher's Note: The statements, opinions and data contained in all publications are solely those of the individual author(s) and contributor(s) and not of MDPI and/or the editor(s). MDPI and/or the editor(s) disclaim responsibility for any injury to people or property resulting from any ideas, methods, instructions or products referred to in the content.